

Slow-release fenobucarb nanofibers: A case study on field efficacy against brown planthopper in rice cultivation in Vietnam

Liem Thanh Nguyen^{1*}, Vu Anh Doan¹, Tuan Anh Phung¹

¹ School of Materials Science and Engineering, Hanoi University of Science and Technology, Hanoi, Vietnam

* Corresponding author e-mail: liem.nguyenthanh@hust.edu.vn

ABSTRACT

Polylactic acid nanofibers encapsulating the insecticide fenobucarb were fabricated by coaxial electrospinning and evaluated for structure, release, and field efficacy in rice. The nanofibers showed an average diameter of 582.12 ± 108.49 nm with 47.175% fenobucarb loaded. In vitro, fenobucarb release reached 22.78% at day 5 and 43.19% at day 15, fitting the Korsmeyer Peppas model ($n = 0.6014$), indicating both profenofos diffusion and the swelling of the polylactic acid shell. Three formulations suspension concentrate, wettable powder, and granule were prepared from the nanofibers scaffolds and applied at 250 g a.i. ha⁻¹ in Bac Giang province, Vietnam. No phytotoxicity was detected. Both suspension concentrate and wettable powder reduced brown planthopper densities from 27 insects hill⁻¹ to 4.3–4.5 insects hill⁻¹ by 15 days after treatment, with efficacy of 86.1 ± 86.8%, outperforming the commercial reference Bassa 50 EC (64.9%). Granule exhibited slower onset but extended activity. Compared with conventional formulations, polylactic acid encapsulation enhanced persistence and bioefficacy, suggesting a practical strategy to lower insecticide input and environmental exposure in rice ecosystems.

Keywords: pesticide, field trial, fenobucarb, rice, nano-formulation.

INTRODUCTION

Agriculture across Asia increasingly relies on chemical pesticides to secure yields, but this reliance is especially pronounced in Vietnam. National statistics indicate that pesticide consumption has reached about 16.5 kg per hectare, the highest in Southeast Asia and several times greater than in Thailand or Cambodia [Hughes et al., 2021]. While these compounds are intended to protect crops, less than 1% of applied pesticides reach target organisms, with the remainder dispersing into soil, water, and air [Tudi et al., 2021; Elhamalawy et al., 2024]. Such inefficiencies result in wide-ranging ecological consequences and prolonged use certainly leads to the accumulation of their persistent residues in the soil. This can cause contamination of agricultural products and the environment [Lishchuk et al., 2024].

Pesticides have been shown to reduce the diversity and ecological function of soil invertebrates, limit humus formation and carbon

sequestration, and disrupt natural enemies, thereby fostering greater dependency on chemicals [Albou et al., 2024; Mohsin et al., 2024]. Globally, it is estimated that millions people are exposed to pesticide residues in surface waters [Chen et al., 2024]. Farmers are particularly vulnerable: more than 30% report acute symptoms after spraying including headaches, skin irritation, and respiratory issues with long-term risks of endocrine disruption, cancer, and neurological disorders [Thi et al., 2018; Moreira et al., 2024].

To address these challenges, nanopesticides have emerged as a promising alternative. These formulations incorporate active ingredients engineered at the nanoscale, enhancing solubility, bioefficacy, and stability while enabling targeted delivery to pests [Belay et al., 2024; Mahleh et al., 2024]. By reducing degradation and lowering required dosages, nanopesticides can cut costs, minimize environmental residues, and improve overall pest management efficiency. They are increasingly viewed as an important tool for sustainable,

eco-friendly agriculture and safe food production [Vandna et al., 2025; Kariyanna et al., 2025].

Experimental evidence supports their potential, Rao et al. (2025) demonstrated that Cry1Ac proteins loaded onto magnesium hydroxide nanoparticles improved leaf adhesion by 59% and increased insecticidal efficacy by 75%, with some nanocarriers also incorporating pH, light, or enzyme responsive release mechanisms [Rao et al., 2018; Sabry et al., 2025].

Advances in nanotechnology further extend to innovative delivery platforms such as electrospinning. This technique uses high voltage electric fields to produce polymer nanofibers with diameters of tens to hundreds of nanometers. Electrospinning setups are relatively simple, comprising a syringe pump, high voltage source, metallic collector, and the method is adaptable to a wide variety of polymers [Rao et al., 2018; Wenjie et al., 2022].

Natural polymers such as alginate and gelatin, as well as synthetic polymers, have been successfully electrospun. In particular, coaxial electrospinning enables the creation of core/shell fibers, allowing for controlled release profiles of encapsulated pesticides [Colín et al., 2024]. Recent research confirms that electrospun nanofibers can protect active agents against degradation by light, temperature, and pH, while reducing dosages and limiting environmental impacts [Samali et al., 2024; Ganesan et al., 2022].

A growing number of field studies highlight the promise of nanopesticides in rice systems. Shakthi et al., (2025) reported a hydrophilic unimolecular nanopesticide of 3 nm formulated with ionic liquids that penetrated insect cuticles and leaf surfaces efficiently, achieving superior pest control compared with commercial formulations while reducing residues and minimizing risks to non-target organisms.

Saby et al. developed chitosan nanoparticle formulations of chlorfenapyr and emamectin benzoate for controlling *Tetranychus urticae* in cucumbers, yielding six and threefold increases in toxicity, mite control rates, and shortened pre-harvest intervals relative to conventional pesticides. In rice, treatment of seeds with a fungicidal nanoparticle achieved *Fusarium fujikuroi* control. Similarly, green synthesized silver-copper nanocomposites demonstrated antibacterial inhibition zones and high fungal control efficacy with potential application against bacterial leaf blight and sheath blight [Zhang et al., 2024; Sabry et al., 2025]. Together, these studies illustrate the transformative

potential of nano pesticides to improve efficacy, reduce chemical residues, and protect beneficial organisms while mitigating environmental impacts. However, challenges remain in assessing long-term ecological safety, biodegradability, and cost-effectiveness. Despite promising laboratory and greenhouse results, large-scale field trials and economic analyses are still limited [Islam et al., 2024; Oluwatoyin et al., 2025].

In Vietnam, pesticide overuse in rice cultivation remains a pressing issue. As the country's most important staple crop, rice occupies the majority of cultivated land and plays a central role in food security. Conventional pesticides such as fenobucarb, hexaconazole, propiconazole are widely applied. While these inputs offer short-term yield benefits, their heavy use contributes to pollution, pest resistance, and health risks for farming communities. Sustainable agricultural development therefore requires strengthened risk management and stricter regulation of pesticide production and packaging [Song et al., 2021; Valérie et al., 2025].

The brown planthopper (*Nilaparvata lugens*) remains a key constraint in rice production in Vietnam due to its direct feeding damage and role as a vector of viral diseases. Among chemical options, fenobucarb has been extensively adopted by farmers, acting through acetylcholinesterase inhibition to suppress planthopper populations. As a member of the carbamate insecticide group, fenobucarb (2-sec-butylphenyl-N-methylcarbamate) is often applied in agricultural systems. In developing countries, these chemicals are commonly applied by farmers in agriculture, especially for crops such as rice, vegetables, and fruits.

Profenofos is used to control a variety of pests including brown planthoppers, green leafhoppers, leaf rollers, armyworms, thrips, semi-loopers, stem borers, and maggots. Rice farming relies heavily on this compound for suppressing destructive pests, particularly the brown planthopper and white-backed planthopper. By blocking acetylcholinesterase activity, fenobucarb interferes with neural signaling in insects, which ultimately results in their death.

This research introduces a novel application of coaxial electrospinning for the fabrication of core/shell microfibers, in which polylactic acid (PLA) functions as the shell matrix while fenobucarb (BPMC) is encapsulated in the core. The electrospun scaffolds were subsequently engineered into three distinct nano-pesticide formulations

and tested for their effectiveness against brown planthoppers in rice cultivation.

By combining a biodegradable polymer carrier with a conventional insecticide, this approach provides an innovative strategy that enhances controlled release, minimizes off-target losses, and reduces environmental risks. The study therefore demonstrates not only the practical potential of this method for rice pest management but also its broader implications for advancing sustainable pesticide delivery technologies.

MATERIAL AND METHODS

Materials

Polylactic acid (PLA, Resomer® R203H, Mw 18,000–24,000, density 1.24 g/cm) was obtained from Sigma-Aldrich. Chloroform, N,N-dimethylformamide and Toluene were supplied by Xilong Scientific Co., Ltd. (China), were employed as solvents. All reagents were of analytical grade. Fenobucarb (98%, density 1.46 g/cm³) was purchased from DC Chemical Co., Ltd. (China). For comparison, BASSA 50 EC (containing 500 g/L profenofos) was provided by Syngenta Co., Ltd. (Vietnam) and used as a reference pesticide formulation.

Another reagents for producing nano-formulated pesticide products included tristyrylphenol ethoxylates (viscosity 920 cps), alkyl naphthalene sulfonate (39.2%, unsulfonated oil content < 1.25%), nano silica (99.7%, particle size 200 nm), sodium lignosulfonate (density of 0.5 g/cm³), lauryl sodium sulphate (T_m 206 °C, water soluble), emulsifying agent Vanzan NF (viscosity

1400–1600 mPa·s, particle size 180 µm), dry sand and kaolin, all sourced from Xilong Scientific Co., Ltd. (China). All chemicals were utilized without further purification.

Preparation of BPMC/PLA electrospun

To prepare the shell solution, 10 g of poly-lactic acid was added to 90 ml of the a chloroform/N,N-dimethylformamide mixed solvent (75:25 by weight) and stirred with a magnetic stirrer at approximately 40 °C until completely dissolved to get 10.0 wt.% polylactic acid solution. The core solution consisted of toluene solvent mixed with the BPMC (98%) to obtain a 30% concentration. Nanofiber scaffolds of BPMC/PLA were fabricated through the coaxial electrospinning of the aforementioned prepared solutions. After the core and shell solutions were cooled down to room temperature, the solutions were transferred to a 5 mL syringe connected with the stainless-steel coaxial spinneret (22 gauge).

According to the previously studied fabrication conditions [Vu et al., 2025], the electrospinning parameters for producing BPMC/PLA nanofibers were selected as follows: core/shell flow rates of 0.18/0.6 mL/h, an applied voltage of 16 kV, and a tip-to-collector distance of 16 cm. All experiments were conducted at ambient conditions of 25 ± 2 °C and 50% relative humidity. The coaxial electrospinning process was conducted for 2 h to obtain the BPMC/PLA nanofiber scaffolds. A flowchart illustration of preparation of BPMC/PLA nanofiber scaffolds, producing nano fomulated and rice field trial is presented in Figure 1.

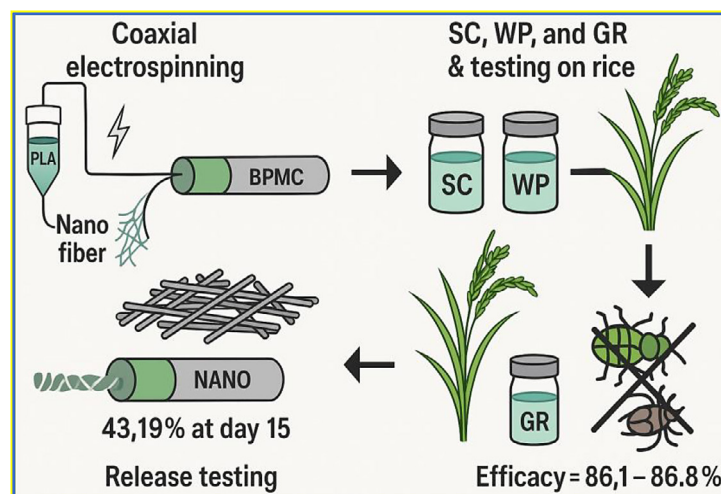


Figure 1. Flowchart of the fabrication and testing process of nano pesticide

Preparation of the nano-pesticide products from BPMC/PLA nanofibers

Three nano-formulated pesticide types were developed based on a nanofibrous scaffold consisting of BPMC as the core and PLA as the shell, serving as the carrier matrix for encapsulating the active ingredient. The formulations were designed in accordance with the TCVN 12561:2022 (Vietnam National Standard) which aligns with FAO/WHO guidelines for pesticide preparation and evaluation. Each formulation was produced with specific ratios of raw materials, including the active pesticide encapsulated within the BPMC/PLA scaffold (Table 1).

For the suspension concentrate (SC) nano-pesticide formulation, BPMC/PLA nanofibers and sodium lignosulfonate (dispersing agent) were dispersed in water within a reactor and pre-mixed at 600 rpm to form an initial suspension. Sodium lauryl sulphate as surfactant was then incorporated, and the mixture was stirred at 1000 rpm for 60 min. The dispersion was subsequently ground to obtain the required particle size, after which suspending agent Vanzan NF was introduced. Final homogenization was performed for 2 h at approximately 1000 rpm.

For the wettable powder (WP) nano-pesticide formulation, tristyrylphenol ethoxylates as dispersing agent, alkyl naphthalene sulfonate as surfactant, and anti-caking agent nano-silica were initially combined in a mechanical mixer for 5 min. BPMC/PLA nanofibers were then added, and mixing was continued for an additional 15 min. The resulting mixture was processed in a disc mill at 1500 rpm for 60 min to achieve a particle size

smaller than 10 μm . For the Granules (GR) nano-pesticide formulation, the raw materials were weighed according to the prescribed formulation. The dispersing agent tristyrylphenol ethoxylates, the surfactant alkyl naphthalene sulfonate, and the solvent were pre-mixed in a mixer for 5 min, after which nano-fibers containing the active ingredient profenofos were incorporated and mixing was continued for 15 min. Water was subsequently added to the mixture, which was homogenized and sprayed onto the surface of the carrier (dry sand), followed by thorough blending in the mixer. The final mixture was dried until the moisture content was reduced to below 3%.

Characterization of BPMC/PLA scaffolds

The morphology of the nanofibers was observed by a scanning electron microscopy (SEM - JSM 6510LV). For statistical reliability, 100 fibers were randomly selected from the SEM images to determine average diameter and distribution.

Chemical structure analysis was carried out using attenuated total reflectance Fourier-transform infrared spectroscopy (ATR-FTIR, Nicolet iS20). Spectra of pure BPMC and BPMC/PLA nanofiber scaffolds were collected in the wavelength range of 4000–500 cm^{-1} , with 64 scans at a resolution of 4 cm^{-1} .

The BPMC content in the nanofibers, or the release level of BPMC at the survey time, was quantified by gas chromatography (GC-6890N Agilent, USA). The BPMC concentration was determined by gas chromatography with a flame ionization detector (FID). Etofenprox was used as the internal standard. Approximately 10 mg of

Table 1. Formulation composition for nano pesticides (SC, WP, GR)

Components	Weight ratio, %		
	SC	WP	GR
BPMC/PLA nanofibers	25	25	10
Tristyrylphenol Ethoxylates	-	4	2
Alkyl Naphthalene Sulfonate	-	3	2
Nano silica	-	2	1
Kaolin	-	66	-
Dry sand	-	-	82
Sodium lignosulfonate	4	-	-
Lauryl sodium sulphate	4	-	-
Vanzan NF	3	-	-
Water	64	-	3
Total	100	100	100

BPMC/PLA nanofiber scaffolds were randomly collected and dissolved in 10 mL of chloropicrin using an ultrasonic bath until complete homogenization was achieved. The resulting solutions were analyzed to quantify the amount of BPMC content as showed in Equation 1.

$$BPMC (\%) = \frac{m \text{ BPMC in scaffold}}{m \text{ dry scaffold}} \times 100 \quad (1)$$

At intervals of days, the amount of *BPMC* released was calculated and the release kinetics were expressed as a function of time *t* (Equation 2).

$$\text{Release \% (t)} = \frac{M_t}{M_n} \times 100\% \quad (2)$$

In Equation 2, M_t (mg) is the weight of BPMC released at each time interval and M_n (mg) is the weight of BPMC loaded in the BPMC/PLA nano-fiber scaffolds.

Mathematical models

In order to distinguish the mechanism of BPMC released from scaffolds, the data of the experimental BPMC release were described by the Korsmeyer-Peppas kinetic models. In this model, the release rate constant (*k*) and the diffusion exponent (*n*), known as the Korsmeyer-Peppas coefficient, are derived from the ratio of the cumulative amount of BPMC released at a given time (M_t) to the initial active ingredient content (M_0) (Eqation 3).

$$\frac{M_t}{M_0} = kt^n \quad (3)$$

where: M_t is the amount of BPMC released at time *t*, M_0 is the initial amount of BPMC, *k* is the kinetic constant characteristic of the material system, *n* is the diffusion exponent indicating the release mechanism.

Field trial under actual field conditions

The field experiment block design and test location are showed in Figure 2. A small scale field trial was carried out in Xuan Phu commune, Bac Giang province, Vietnam, from 13 June to 28 June 2025. Each experimental block measured 360 m² and was arranged sequentially without replication.

To minimize external interference, one meter buffer zone separated adjacent plots, and the entire test area was positioned at least 1.0 m from the field boundaries. The site was located at 21.23806° N, 106.26139° E, with an elevation of 60 m above sea level. The test crop was direct-seeded rice (Thu Do) at the growth stage of grain-filling ripening (milk to dough stage, when the grains are firming up and the husks begin turning yellow at the tips).

Soil at the site was classified as light loam. For each plot, fertilization included 360 kg of farmyard manure, 21.6 kg of lime, 5.4 kg of urea, and 5.4 kg of potassium sulfate. The field was managed under a rotation system with other short duration crops.

At the time of spraying, brown planthoppers were causing damage and tended to increase in population. During the trial, weather conditions were favorable: on the day of pesticide application, temperatures ranged between 26–32 °C with sunny skies, no rain and light winds, while the following days were showers with rainfall ranging from 15 mm to 35 mm each time, temperature 24–36 °C and the humidity 60–95%.

The target pest for the field trial was the early brown planthopper (1st - 2nd instars), which were actively emerging and infesting the rice crop with a steadily increasing population density (25.5–27.6 insects per rice hill). No additional harmful

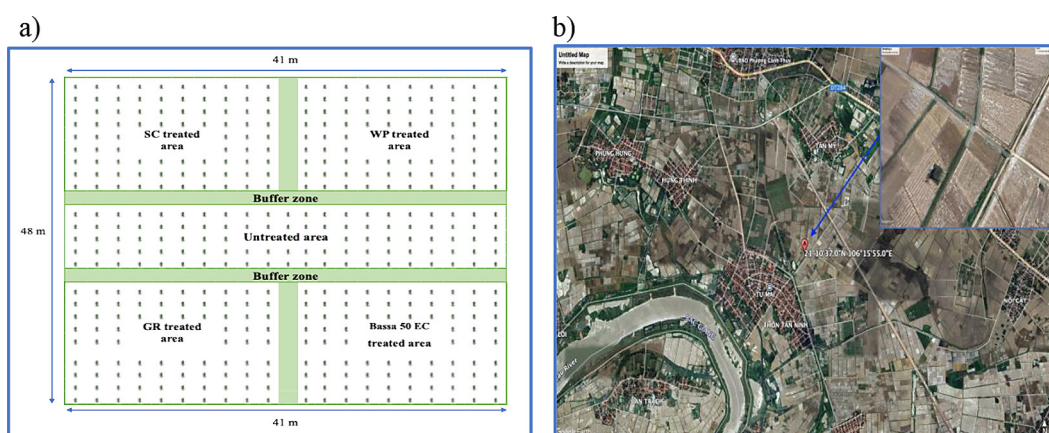


Figure 2. Field experiment block design (a), Test location at Bac Giang, Vietnam (b)

organisms were detected in the experimental plots. The effectiveness (E%) was calculated using Abbott's formula (Abbott, 1925), which calculates efficacy based on larval population density recorded during each survey (Equation 4).

$$E (\%) = \frac{C_{ctr} - C_{trt}}{C_{ctr}} \times 100 \quad (4)$$

where: E – Effectiveness of the tested pesticide, (%), C_{ctr} – Value observed in the control sample (untreated), C_{trt} – Value observed in the treated sample.

RESULTS AND DISCUSSION

Chemical characteristic and morphology of BPMC/PLA nanofiber scaffolds

The chemical composition and morphology of BPMC/PLA microfibers were determined using Fourier-transform infrared spectroscopy (FTIR) and scanning electron microscopy (SEM). The results are presented in Figure 3 and Figure 4. Infrared spectra of BPMC, pristine PLA, and electrospun BPMC/PLA nanofibers were recorded, as shown in Figure 3.

In the FTIR spectrum of BPMC, characteristic absorption bands were observed at ~ 3320 cm^{-1} (N–H stretching of the carbamate group) and 1250 cm^{-1} (C–O–C stretching of the carbamate). Notably, these signals were absent in the BPMC/PLA spectrum, suggesting that no detectable BPMC remained on the fiber surface. In contrast, the BPMC/PLA fibers exhibited strong absorption bands at 1080 cm^{-1} , 1745 cm^{-1} , and

2995 cm^{-1} , corresponding to C–O–C stretching (ester), C=O stretching (ester carbonyl), and C–H stretching ($-\text{CH}_3$, $-\text{CH}-$) vibrations, which are characteristic of pristine PLA. These findings confirm that the infrared response of the composite fibers is dominated by PLA, with no apparent surface contribution from BPMC.

Figure 4 indicated that the resulting BPMC/PLA nanofibers exhibit both the small and consistent diameters. The fiber diameters range from 300 nm to 1100 nm, with a mean diameter of 582.12 nm and a variation of 108.49 nm.

From the SEM images, it can be observed that the fiber size is not uniform. This can be explained by the fact that the outer shell (PLA) contains a large amount of solvent (PLA 10% wt.), while the core has a lower solvent content (BPMC 30% wt.). As a result, under the applied voltage and due to the viscosity difference between the core and the shell, the core stream flows out more slowly and is less stretched, leading to an increase in the overall fiber diameter, making the fibers thicker and non-uniform

In vitro BPMC release profiles and release kinetics

In vitro BPMC release profiles and BPMC content in BPMC/PLA nanofiber scaffolds were showed in Figure 5. The total amount of BPMC in the nanofiber mat was calculated as shown in Equation 1. The BPMC loaded in nanofiber could be as high as 47.175% (Figure 6a). Under the fabrication conditions and the respective solution concentrations as above mentioned, the BPMC

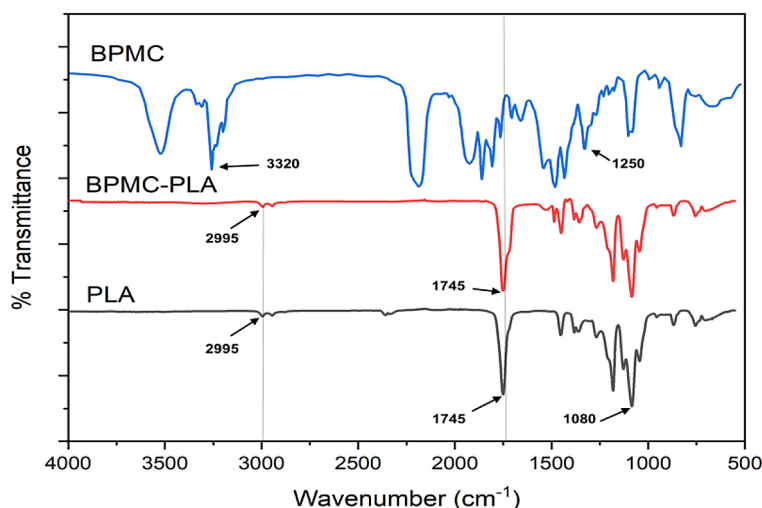


Figure 3. Infra spectra of virgin BPMC, neat PLA and BPMC/PLA nanofiber

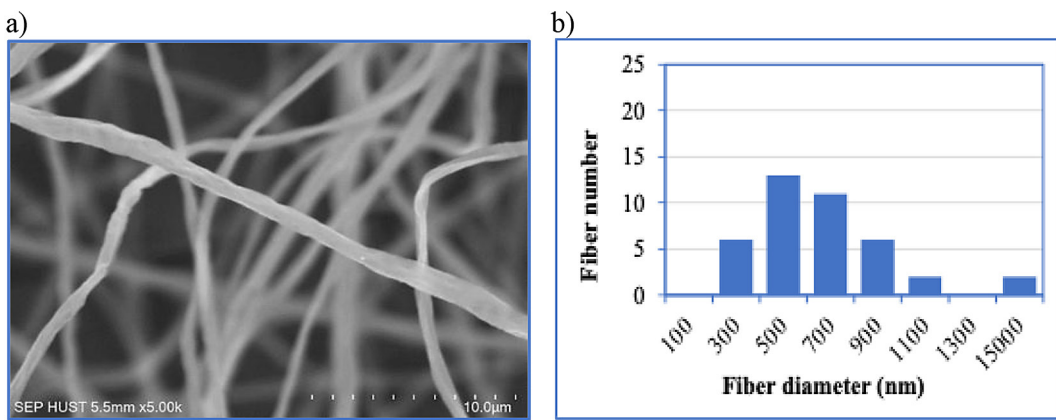


Figure 4. SEM images of BPMC/PLA nanofibers (a), BPMC/PLA scaffolds

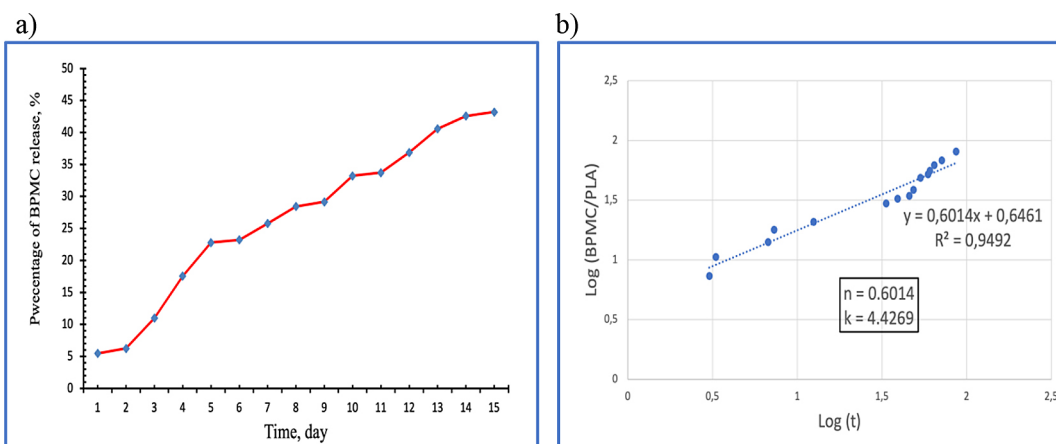


Figure 5. BPMC release rate from BPMC/PLA nanofiber (a), Release profile curve (b)

content encapsulated within the nanofibers can theoretically reach 47.368% (0.4074% loss). This behaviour can be attributed to the loss of BPMC due to solvent evaporation during the fiber formation process. The results from Figure 5a demonstrate that BPMC/PLA nanofiber scaffolds exhibited a sustained BPMC-release profiles. A slow release of BPMC was observed during the first 2 days (first lag time).

It can be explained that the hydrophobicity of the PLA outer layer requiring a long time for water permeation. When the scaffold was wetted, in this case is after 2 days, the BPMC released faster, and reaching approximately 22.78 % of the loaded BPMC in 5 days and reached at 43.19 % after 15 days. A recurrence of lag time was notably observed on days 5–6 and 10–11 (second and third lag time), which may be attributed to the hardly diffused out BPMC embedded in the core region of the nanofibers.

In order to study the mechanism of BPMC release from BPMC/PLA nanofiber scaffolds, the

release data were fitted to the Korsmeyer-Peppas kinetic models. The regression equations and parameters determined by fitting the BPMC release data to mathematical models is shown in Figure 5b. The results in Figure 5b showed that the value of n determined by the Korsmeyer-Peppas model was of 0.6014, in the range of 0.43 ÷ 0.89, which means that the BPMC release mechanism could be represented by an anomalous diffusion. Such behaviour suggests that the release process is jointly governed by Fickian diffusion and PLA swelling, involving both the BPMC encapsulated in the core and the PLA shell matrix.

Field trial under field conditions

For comparison, the commercial formulation Bassa 50 EC served as a reference standard and a test plot untreated with any pesticides only sprayed with water to serve as the control area. Liquid treatments were applied by thoroughly spraying the rice canopy with 18-liter electric

backpack sprayers. To avoid confounding effects, no additional plant protection products were used during the trial.

Efficacy assessments for each treatment were conducted at 10 sampling points arranged along two diagonal transects within the test plot. To minimize border effects, each sampling point was positioned 1 m from the plot edge. Survey 10 points along the two diagonals of the experimental plot. At each point, use a 20 × 40 cm oil-coated tray to collect samples (rotate the tray to four sides and make two taps on each side). Brown planthopper density was then calculated as the average number of brown planthopper per plant.

To accurately determine the application dose, the BPMC content in the products after fabrication was quantified by the GC assay described above. The results showed that the actual BPMC contents in the SC, WP, and GR formulations were 11.065%, 10.15%, and 4.56%, respectively (Figure 6).

The deviation from the calculated values may be due to the actual BPMC content present in the nanofiber used to prepare the formulations, and

losses during production. Based on the determination of active ingredient content in the SC, WP and GR formulations, and following the Vietnam national standard requirement of 250 g of active ingredient (BPMC) per hectare, the application dosage for each treatment was established, as summarized in Table 2.

The results of efficacy evaluations for BPMC loaded nanofibers, as well as their effects on rice plants at different intervals after treatment, are summarized from Tables 3 to Table 5. Treatments were applied to rice, and conducting an examination of the effects of the BPMC starting from the beginning of spraying, with inspections carried out every two days.

The evaluation of the effects of BPMC on the growth and development of rice was carried out using a grading scale from level 1 (the plant shows no signs of toxicity), level 2 (mild toxicity with slight growth reduction detectable upon close inspection), level 3 (clear toxicity symptoms easily visible to the naked eye) to level 9 where the rice plant is completely dead.

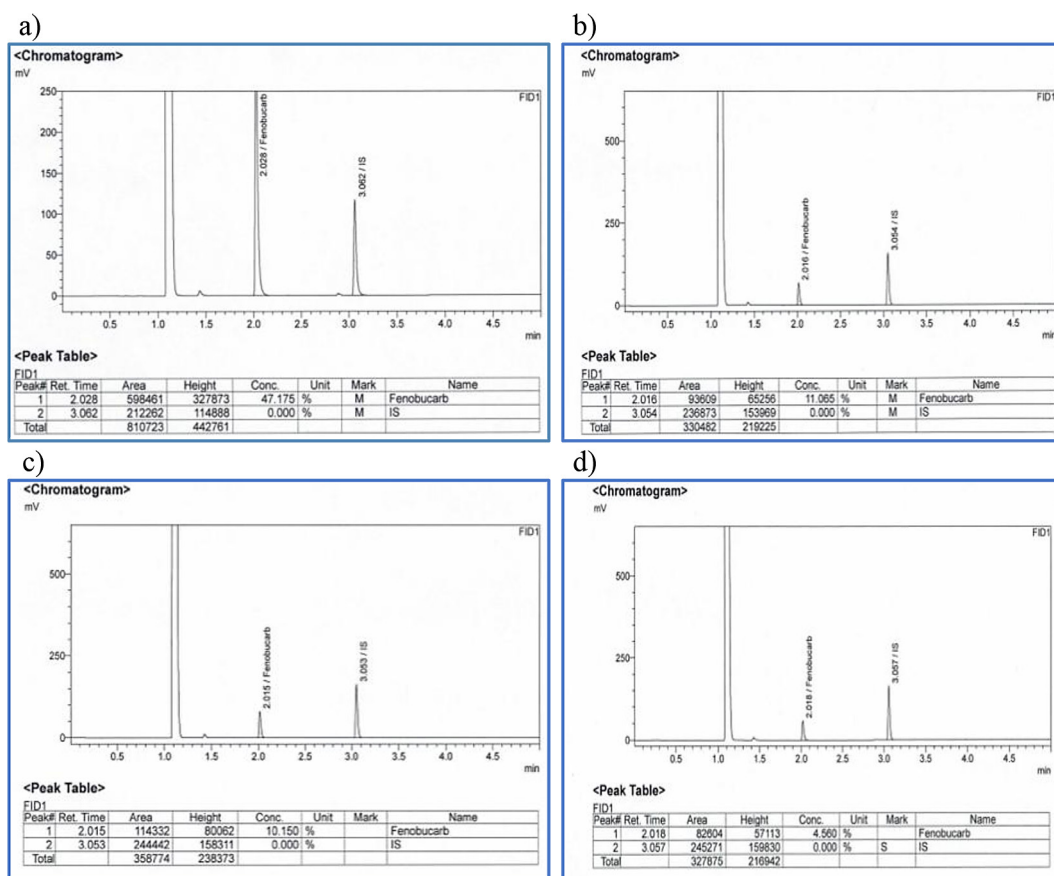


Figure 6. BPMC loaded content: (a) in BPMC/PLA nanofiber scaffolds, (b) in SC formulation, (c) in WP formulation, (d) in GR formulation

Table 2. Treatment conditions

No.	Treatments	Dose/ha		Dilution in water/ ha
		Technical g a.i. /ha	Formulation g/ha	
1	SC product	250	2259.38	500 L
2	WP product	250	2463.05	500 L
3	GR product	250	5482.46	500 L
4	Bassa 50EC	250	500	500 L
5	Untreated	0	0	0

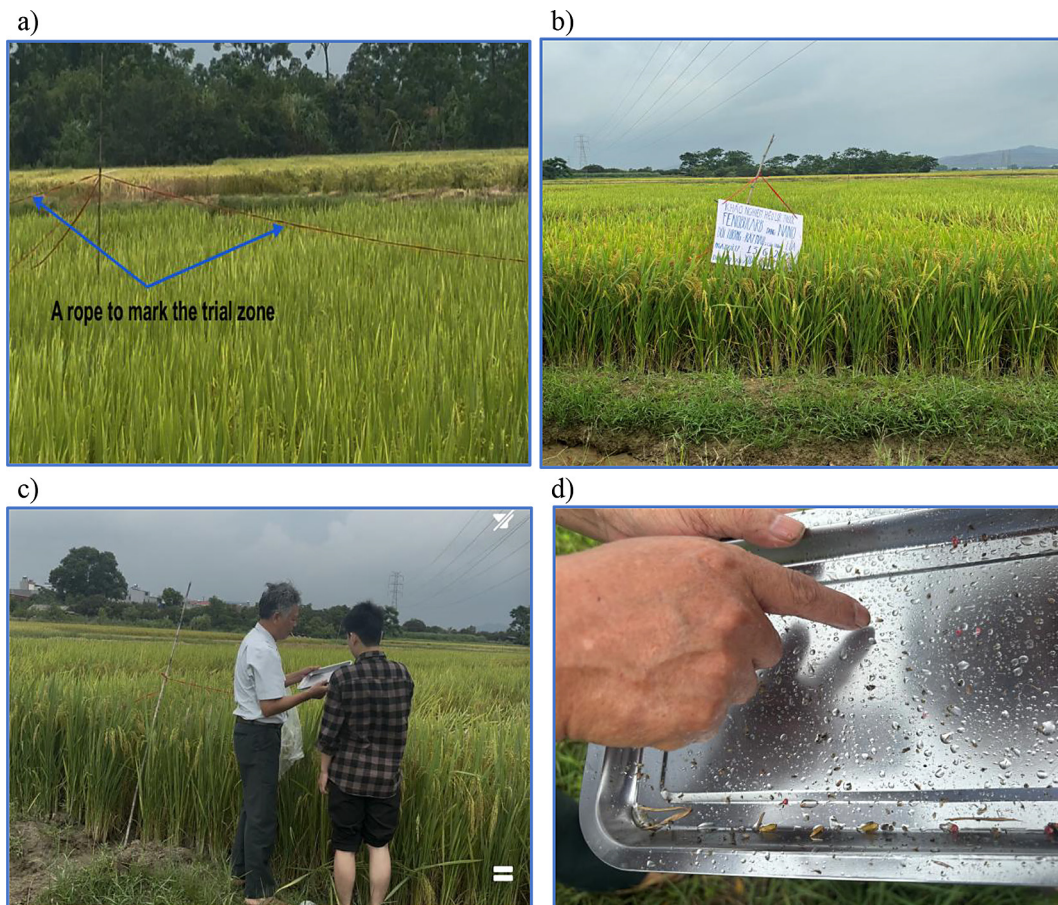


Figure 7. Field trial under field conditions: (a) after 15 days spray, (b) about to harvest rice, (c) Prepare trays for determining the density of brown planthoppers on rice, (d) the tray

Across all assessment periods, rice plants treated with the suspension concentrate (SC), wettable powder (WP), granules (GR) and the reference formulation Bassa 50EC exhibited no observable phytotoxicity. This indicates that the tested nano-formulations were safe for rice under the experimental conditions.

To evaluate the efficacy of the BPMC treatments against brown planthopper, periodic field surveys were carried out to record brown planthopper survival at different observation intervals. Brown planthopper per plant was

calculated by dividing the number of live brown planthopper observed by the total number of plants examined. The survey outcomes, representing changes in brown planthopper population density under each treatment, are showed in Tables 4 and Table 5.

From the results presented in Table 4, it is evident that the population of brown planthoppers tended to decline following application of the SC and WP formulations. After 15 days, their densities decreased markedly from 27 insects per hill to 4.5 and 4.3 insects per hill, respectively.

Table 3. Effects on rice plants after treatment

No.	Treatments	Toxicity level							
		1 DAT	3 DAT	5 DAT	7 DAT	9 DAT	11 DAT	13 DAT	15 DAT
1	SC product	1	1	1	1	1	1	1	1
2	WP product	1	1	1	1	1	1	1	1
3	GR product	1	1	1	1	1	1	1	1
4	Bassa 50EC	1	1	1	1	1	1	1	1
5	Untreated	1	1	1	1	1	1	1	1

Note: DAT – days after treatment.

For both SC and WP, the most pronounced reduction occurred within 5 days after spraying. This observation can be attributed to the high release rate of the active ingredient at 15 days (Figure 7), governed by diffusion and PLA swelling mechanisms.

In contrast, the GR formulation showed an opposite trend, with planthopper densities increasing after 11 days of application. This may be explained by the lower immediate efficacy of granules compared to foliar sprays. Since GR was applied to the water surface and taken up gradually through the rice roots before being translocated within the plant, its activity was mainly expressed against younger planthopper stages. A similar increase in planthopper density was observed at 13 days after GR treatment.

A decline in planthopper numbers was also observed with the reference product Bassa 50EC. However, from day 9 onwards, the population tended to rise again, reaching 11.4 insects per

hill. This may be due to reduced persistence of the insecticide under field conditions, where high temperature and solar radiation accelerate degradation.

Table 5 presents the effectiveness of the tested BPMC formulations compared with the untreated control. Both SC and WP provided higher and faster efficacy than GR, achieving more than 50% effectiveness after only 5 days. By contrast, GR was slower, reaching only 43.24% effectiveness at the same interval. Nevertheless, all three formulations eventually reached over 70% effectiveness (86.15% for SC, 86.77% for WP, and 72.31% for GR). Meanwhile, the commercial product Bassa 50EC showed a decline in effectiveness after 7 days, and by day 15 its activity was reduced to 64.92%. This decline can be explained by the fact that Bassa 50EC contains unprotected BPMC, which is prone to degradation by temperature and sunlight. In comparison, the newly

Table 4. Density of surviving brown planthopper across survey periods

No.	Treatments	Density, brown planthopper/plant								
		DBT	1 DAT	3 DAT	5 DAT	7 DAT	9 DAT	11 DAT	13 DAT	15 DAT
1	SC product	27.2	16.6	13.2	9.8	9.4	6.5	6.3	4.7	4.5
2	WP product	26.3	18.7	15.2	12.8	11.1	8.3	7.7	4.9	4.3
3	GR product	27.6	20.6	16.7	14.7	9.2	8.5	7.9	8.1	9.0
4	Bassa 50EC	26.9	9.5	6.8	5.6	5.4	5.9	7.5	10.2	11.4
5	Untreated	26.5	26.8	24.1	25.9	25.3	27.5	29.1	31.2	32.5

Note: DBT – days before treatment.

Table 5. Efficacy of the BPMC across survey periods

No.	Treatments	Effectiveness of the tested BPMC, E (%)							
		1 DAT	3 DAT	5 DAT	7 DAT	9 DAT	11 DAT	13 DAT	15 DAT
1	SC product	38.06	45.23	62.16	62.85	76.36	78.35	84.94	86.15
2	WP product	30.22	36.93	50.58	56.13	69.82	73.54	84.29	86.77
3	GR product	23.13	30.71	43.24	63.64	69.09	72.85	74.04	72.31
4	Bassa 50EC	64.55	71.78	78.39	78.66	78.55	74.23	67.31	64.92

developed SC, WP, and GR formulations encapsulated BPMC within a PLA matrix, which provided a protective barrier against environmental stress and allowed for sustained release after application in rice fields.

CONCLUSIONS

Core-shell nanofibers containing fenobucarb (BPMC) with a PLA shell and BPMC core were successfully fabricated, exhibiting an average diameter of approximately 500 nm. Using these nanofibers, three novel nanoformulations were developed: suspension concentrate (SC), wettable powder (WP), and granule (GR). Field trials on rice confirmed that all three formulations were effective against brown planthoppers, with SC and WP demonstrating faster and stronger initial control, while GR provided more gradual protection through root uptake.

Compared with the commercial product Bassa 50EC, the nano formulations achieved higher and more sustained efficacy, highlighting the protective role of the PLA matrix against environmental degradation and its ability to enable controlled release of BPMC. These findings suggest that PLA based nanofiber encapsulation is a promising approach for improving the performance and persistence of fenobucarb in rice pest management, offering both enhanced efficacy and greater environmental stability. The superior performance of the BPMC/PLA based formulations can be attributed to the controlled-release properties conferred by the PLA encapsulation. This dual mechanism allows for the gradual release of BPMC from the core while the PLA shell acts as a physical barrier against environmental stressors such as UV radiation and thermal degradation. As a result, the active ingredient is better preserved, enabling extended field efficacy compared to conventional formulations.

Further studies should focus on scaling up the production of PLA based nanofibers and evaluating their cost-effectiveness under large-scale field conditions. In addition, long-term ecological impacts and residue behavior of these nanoformulations should be investigated to ensure environmental safety and regulatory compliance. Finally, this encapsulation strategy could be extended to other insecticides, broadening its applicability in sustainable pest management.

Acknowledgment

The authors would like to sincerely thank the Functional Polymer Laboratory – HUST for providing measurement equipment support for this research, Mr. Vu Van Vu (Northern Plant Protection Drug Inspection and Testing Center, Hanoi, Vietnam), and Mr. Tao Minh Tuan (Center for Research and Consulting on the Development of Plant Protection Drugs and Fertilizers) for their assistance in preparing the pesticide and conducting field trials.

REFERENCES

1. Albou, E. M., Abdellaoui, M., Abdaoui, A., Ait, B. A. (2024). Agricultural Practices and their Impact on Aquatic Ecosystems: A Mini Review. *Ecological Engineering & Environmental Technology*, 25(1), 321–331. <https://doi.org/10.12912/27197050/175652>
2. Belay, D., Amensisa, H. T., Chala, D., Embay, A. A., Yonas, A., Ahmed, M. E., Tarikuwa, N., Seada, H., Lebasie, W. (2024). Pesticide safe use practice and acute health symptoms, and associated factors among farmers in developing countries: a systematic review and meta-analysis of epidemiological evidence. *BMC Public Health*, 24, 3313. <https://doi.org/10.1186/s12889-024-20817-x>
3. Chen, J., Zhao, L., Wang, B., He, X., Duan, L., Yu, G. (2024). Uncovering global risk to human and ecosystem health from pesticides in agricultural surface water using a machine learning approach. *Environ Int*. 194, 109154. <https://doi.org/10.1016/j.envint.2024.109154>
4. Colín, O., Julia, Elena, C. O., Ricardo, V. B. (2024). Production of nanofibers by electrospinning as carriers of agrochemical. *Fibers*, 12(8). <https://doi.org/10.3390/fib12080064>
5. Doan, V. A., Anh, L. T. H., Phung, T. A., Vu, D. M., Khac, V. T., Nguyen, L. T. (2025). Controlled-release pesticide nanofibers for sustainable agriculture: Effects of processing parameters on fiber morphology and release kinetics. *Journal of Ecological Engineering*, 26(6), 48–61. <https://doi.org/10.12911/22998993/201995>
6. Elhamalawy, O., Bakr, B., Eissa, F. (2024). Impact of pesticides on non-target invertebrates in agricultural ecosystems. *Pesticide Biochemistry and Physiology*, 202, 105974. <https://doi.org/10.1016/j.pestbp.2024.105974>
7. Ganesan, A., Rengarajan, J. (2022). A review on fabrication methods of nanofibers and a special focus on application of cellulose nanofibers. *Carbohydrate Polymer Technologies and Applications*, 4, 100262. <https://doi.org/10.1016/j.carpta.2022.100262>
8. Hughes, D., Thongkum, W., Tudpor, K., Turnbull, N., Yukalang, N., Sychareun, V., Vo, T. V., Win, L. L., Watkins, A., Jordan, S. (2021). Pesticides use and health impacts on farmers in Thailand, Vietnam,

and Lao PDR: Protocol for a survey of knowledge, behaviours and blood acetyl cholinesterase concentrations. *Plos one*, 16(9): e0258134. <https://doi.org/10.1371/journal.pone.0258134>

9. Islam, A., Bhuiyan, R., Nihad, S., Akter, R., Khan, M. (2024). Green synthesis and characterization of silver nanoparticles and its efficacy against Rhizoctonia solani, a fungus causing sheath blight disease in rice. *Plos One*, 19(6): e0304817. <https://doi.org/10.1371/journal.pone.0304817>
10. Kariyanna, B., Sowjanya, M. (2025). Unravelling the use of nanotechnology for crop pest management as a green and sustainable agriculture. *The Journal of basic and applied Zoology*. 86, 51. <https://doi.org/10.1186/s41936-025-00459-0>
11. Li, X., Wang, X., Sun, C. (2025). A unimolecule nanopesticide delivery system applied in field scale for enhanced pest control. *Nat Commun*, 16, 6809. <https://doi.org/10.1038/s41467-025-61969-7>
12. Lishchuk, A., Parfenyk, A., Furdychko, O., Bordonay, V., Beznosko, I., Drebota, O., Karachinska, N. (2024). Ecotoxicological Hazard of Pesticide Use in Traditional Agricultural Technologies. *Journal of Ecological Engineering*, 25(2), 274–289. <https://doi.org/10.12911/22998993/177275>
13. Mahleh, E., Jakub, H., Jan, K., Renato, G., Zuzaña, H.B., Nicola, R., Sebastian, H. (2024). Nano-enabled pesticides: a comprehensive toxicity assessment of tebuconazole nanoformulations with nematodes at single species and community level. *Environ Sci Eur*, 36, 51. <https://doi.org/10.1186/s12302-024-00879-9>
14. Mohsin, R. I., Alamari, M. J., Jaber, H. H. (2024). The toxicity of organophosphates insecticide in cyprinus carpio and effect on antioxidant and liver function. *Ecological Engineering & Environmental Technology*, 25(7), 244–250. <https://doi.org/10.12912/27197050/188379>
15. Moreira, A., Manuela, V.S. (2024). Analysis of health effects reported by agricultural workers and the adverse human effects indicated on pesticide labels: a systematic review. *Agriculture*, 14(10), 1669. <https://doi.org/10.3390/agriculture14101669>
16. Oluwatoin A. F., Ayorinde V. O., Hector S. M. (2025). Polysaccharide polymer-based nanoparticles for nano fertilizer and nano pesticides: A review. *Carbohydrate Polymer Technologies and Applications*, 2025, 101009. <https://doi.org/10.1016/j.carpta.2025.101009>
17. Rao, W., Zhan, Y., Chen, S., Xu, Z., Huang, T., Hong, X., Zheng, Y., Pan, X., Guan, X. (2018). Flowerlike Mg(OH)₂ cross-nanosheets for controlling Cry1Ac protein loss: Evaluation of insecticidal activity and biosecurity. *J Agric Food Chem.*, 66(14), 3651–3657. <https://doi.org/10.1021/acs.jafc.8b00575>
18. Sabry, A.H., Helmy, R.M.A., Sleem, R.A. (2025). Impact of two nano-pesticide formulations in combating the two-spotted spider mite, Tetranychus urticae Koch, and their residues in cucumber fruits, Cucumis sativus L. *Sci Rep*, 15, 16552. <https://doi.org/10.1038/s41598-025-99726-x>
19. Samali, U. L., Sanjeewa, K. R., Nilwala, K., Venranja, K., Menaka, H., Tharaka, R., Lahiru, U., Dushmantha, A. (2024). Citronella oil-loaded electrospun single and core-shell nano fibers as sustained repellent systems against Aedes aegypti. *Next Nanotechnology*, 7, 100127. <https://doi.org/10.1016/j.nxnano.2024.100127>
20. Shakthi, S., Abhipriya, P., Prasath, V.A., Vivek, K., Hong, W. X. (2025). Innovations in electrospinning techniques for nanomaterial synthesis and its applications in the field of active food packaging. *Journal of Future Foods*. <https://doi.org/10.1016/j.jfutfo.2025.02.010>
21. Song, N., Thuy, N., Tiep, N., Ha, T., Que, N. and Huong, N. (2021). Pesticide risk reduction of vegetable farmers: A case study in Vietnam. *Journal of Environmental Protection*, 12, 1055–1068. <https://doi.org/10.4236/jep.2021.1212062>
22. Thi, H. N., Nguyen, T. P. M., Nam, H., Hoang, T.N. (2018). Paraquat in surface water of some streams in Mai Chau Province, the Northern Vietnam: Concentrations, profiles, and human risk assessments. *Journal of Chemistry*, 8521012. <https://doi.org/10.1155/2018/8521012>
23. Tudi, M., Daniel, R.H., Wang, L., Lyu, J., Sadler, R., Connell, D., Chu, C., Phung, D.T. (2021). Agriculture development, pesticide application and its impact on the environment. *Int J Environ Res Public Health*. 18(3), 1112. <https://doi.org/10.3390/ijerph18031112>. PMID: 33513796; PMCID: PMC7908628.
24. Valérie, F., Jérémie, P., Emmanuel, Fl. (2025). Efficiency and safety of nanopesticides, it takes two to tango. An overview of the lack of data on possible effects on human health. *Science of The Total Environment*, 973, 179156. <https://doi.org/10.1016/j.scitotenv.2025.179156>
25. Vandna, S., Sveta, T. (2025). Green nano-pesticides from plant sources: Synthesis, mechanisms, environmental impacts, and prospects for sustainable agriculture. *Pesticide Biochemistry and Physiology*, 213, 106543. <https://doi.org/10.1016/j.pestbp.2025.106543>
26. Wenjie, S., Shuqi, L., Lidong, C., Min, W., Zishi, W., Hongliang, X. (2022). Electrospinning and nanofibers: Building drug delivery systems and potential in pesticide delivery. *Materials Today Communications*, 33, 104399. <https://doi.org/10.1016/j.mtcomm.2022.104399>
27. Zhang, Q., Shi, X., Gao, T., Xing, Y., Jin, H., Hao, J., Liu, X., Liu, X., Liu, P. (2024). Precision management of Fusarium fujikuroi in rice through seed coating with an enhanced nanopesticide using a tannic acid-Zn^{II} formulation. *J Nanobiotechnology*, 22(1), 717. <https://doi.org/10.1186/s12951-024-02938-y>